

**A Study of Currents Associated with the use of Euler Potentials
to Model the Magnetic Field of Jupiter**

Douglas E. Jones
Brigham Young University,
Provo, Utah

Claudia J. Alexander
Jet Propulsion Laboratory (JPL)
Pasadena, California

Irene M. Engle
Physics Department, U. S. Naval Academy,
Annapolis, Maryland

Abstract

A study of several Harris current sheet type Euler potential models of Jupiters magnetosphere is presented. It is found that in every case the specific functional form and nature of the model coefficients generated in the fitting of data near the equatorial plane produce non-physical currents in the vicinity of the symmetry axis, which in turn cause a severe high latitude distortion of the magnetic field. Although this modeling approach can be used to provide more information regarding the nature of the current sheet distortions, it appears to be unreliable for use in global modeling.

Introduction

Modeling of a planetary magnetosphere has generally utilized two methods for expressing the magnetic field: application of the Biot-Savart Law using specified currents, or use of Euler Functions f and g to express \mathbf{B} , where

$$\mathbf{B}(\rho, \phi, z) = \nabla f(\rho, \phi, z) \times \nabla g(\rho, \phi, z)$$

Such a function automatically satisfies $\text{div } \mathbf{B} = 0$, and proper choice of the f and g functions can result in excellent fits to the data. However, an additional constraint that is needed for a global modelling is that the corresponding curl \mathbf{B} operation provides meaningful currents.

Although excellent fits to the Jupiter magnetic field data along segments of the trajectories of Pioneer 10, and Voyager 1 and 2 have been obtained using an Euler potential representation of a thick current sheet (Goertz et al., 1974; Jones and Melville, 1975; Goertz et al. 1976; Jones et al. 1980; Khurana, 1997), we will show that the anomalous nature of the magnetic field near the symmetry axis, as well as the presence of anomalous currents obtained through curl \mathbf{B} , suggest that this type of Euler potential cannot be used for global magnetospheric modelling.

Recently, through the use of more complex f and g functions, Khurana (1997) has been able to remove the singular nature of the field at $r = 0$ present in the earlier models, and has obtained an improved fit to the data. In addition, considerable insight into the detailed nature of the Jovian current sheet has been provided using this modelling technique. However, in the present study we will show that anomalous fields and currents still exist in the model outside the fitting region, - particularly near the spin axis. It is not surprising, therefore, that studies involving the global nature of such a magnetosphere, - wherein it is necessary to extrapolate the model well outside the fitting region, - are characterized by anomalous behaviour (Engle, 1997).

The Harris Sheet

To date, the Euler potential models for Jupiter all have their basic root in the expression for the Harris current sheet, wherein

$$f = - B_0 D \log \cosh (z/D); \quad g = y$$

Thus, using for the magnetic field, \mathbf{B} , the expression

$$\mathbf{B}(x,y,z) = \nabla f(x,y,z) \times \nabla g(x,y,z)$$

there results

$$\mathbf{B}(x,y,z) = B_0 \tanh (z/D) \mathbf{i}$$

and using $\mu_0 \mathbf{J} = \nabla \times \mathbf{B}(x,y,z)$

$$\mu_0 \mathbf{J} = B_0 D \operatorname{sech}^2(z/D) \mathbf{j}$$

The starting point for the cylindrical version of the Harris current sheet is

$$f = f(\rho,z) = -A(\rho) \ln \cosh(z/D); \quad g = C(\rho,\phi)$$

Thus,

$$\nabla f = - \left[\frac{\partial A(\rho)}{\partial \rho} \right] \ln \cosh(z/D) \boldsymbol{\rho} - [A(\rho)/D] \tanh (z/D) \mathbf{k}$$

$$\nabla g = \frac{\partial C(\rho,\phi)}{\partial \rho} \boldsymbol{\rho} + 1/\rho \frac{\partial C(\rho,\phi)}{\partial \phi} \boldsymbol{\phi}$$

For simplicity, letting $C(\rho,\phi) = \phi$, we have then

$$\mathbf{B} = (1/\rho) \left[\frac{\partial A(\rho)}{\partial \rho} \right] \ln \cosh(z/D) \mathbf{k} + 1/\rho [A(\rho)/D] \tanh (z/D) \boldsymbol{\rho}$$

One of the problems with adapting the Harris sheet to a cylindrical geometry results because the data requires that the field component B_ρ decrease with ρ . Hence, a factor $1/\rho^a$, ($a > 0$) is required to fit the data; thus $\mathbf{B} \Rightarrow \infty$ as $\rho \Rightarrow 0$. Also, it is not possible to use this method to represent an azimuthal disc of current having a non-zero inner radius. Thus, the basic nature of the cylindrical form of the Harris current sheet expression suggests that it can be used to infer the nature of the field and currents only in and near the actual fitting region (assuming $\rho \Rightarrow 0$ is excluded). We next compare the several attempts to use this approach to fit the Jovian magnetic field data.

Jones-Melville Model

The cylindrical coordinate expression for the Euler potential representation of the magnetic field, \mathbf{B} , i.e.,

$$\mathbf{B}(\rho, \phi, z) = \nabla f(\rho, \phi, z) \times \nabla g(\rho, \phi, z)$$

is

$$B_\rho = (1/\rho \partial f / \partial \phi)(\partial g / \partial z) - (\partial f / \partial z)(1/\rho \partial g / \partial \phi)$$

$$B_\phi = (\partial f / \partial z)(\partial g / \partial \rho) - (\partial f / \partial \rho)(\partial g / \partial z)$$

$$B_z = (\partial f / \partial \rho)(1/\rho \partial g / \partial \phi) - (1/\rho \partial f / \partial \phi)(\partial g / \partial \rho)$$

Using a 5 parameter set of f and g functions of the form (Jones and Melville, 1975; see also Goertz et al., 1976 and Jones et al., 1980 for variations involving the use of both ρ and r)

$$f = -(AD/\rho^{a-1})[\ln \cosh(z/D) + 15]; \quad g = k\rho + \phi$$

there results

$$B_\rho = (A/\rho^a) \tanh(z/D)$$

$$B_\phi = -(kA/\rho^{a-1}) \tanh(z/D)$$

$$B_z = [AD(a-1)/(\rho^{a+1})][\log \cosh(z/D) + 15]$$

Thus, with a typically ≈ 0.7 , B_ρ and B_z tend to ∞ as $\rho \rightarrow 0$. Adding this Euler potential field to a centered dipole planetary field results in the field pattern in Figure 1. The rms fit of this model with the Pioneer 10 data is 3.52 nT. However, it is clear that all of the field components are not well behaved in the vicinity of the origin. To explore this type of model further we compute the current density, \mathbf{J} . Using $\mu_0 \mathbf{J} = \nabla \times \mathbf{B}(\rho, \phi, z)$ there results:

$$\mu_0 \mathbf{J} = [(kAD/\rho^{a-1})\text{sech}^2(z/D)]\hat{\rho} + [(AD/\rho^a)\text{sech}^2(z/D)]\hat{\phi}$$

$$+ \{ [AD(a^2-1)/\rho^{a+2}][\log \cosh(z/D)] + (a^2-1)(15AD)/\rho^{a+2} \}\hat{\phi}$$

$$+ \{ [Ak(a-2)/\rho^a][\tanh(z/D)] \}\hat{k}$$

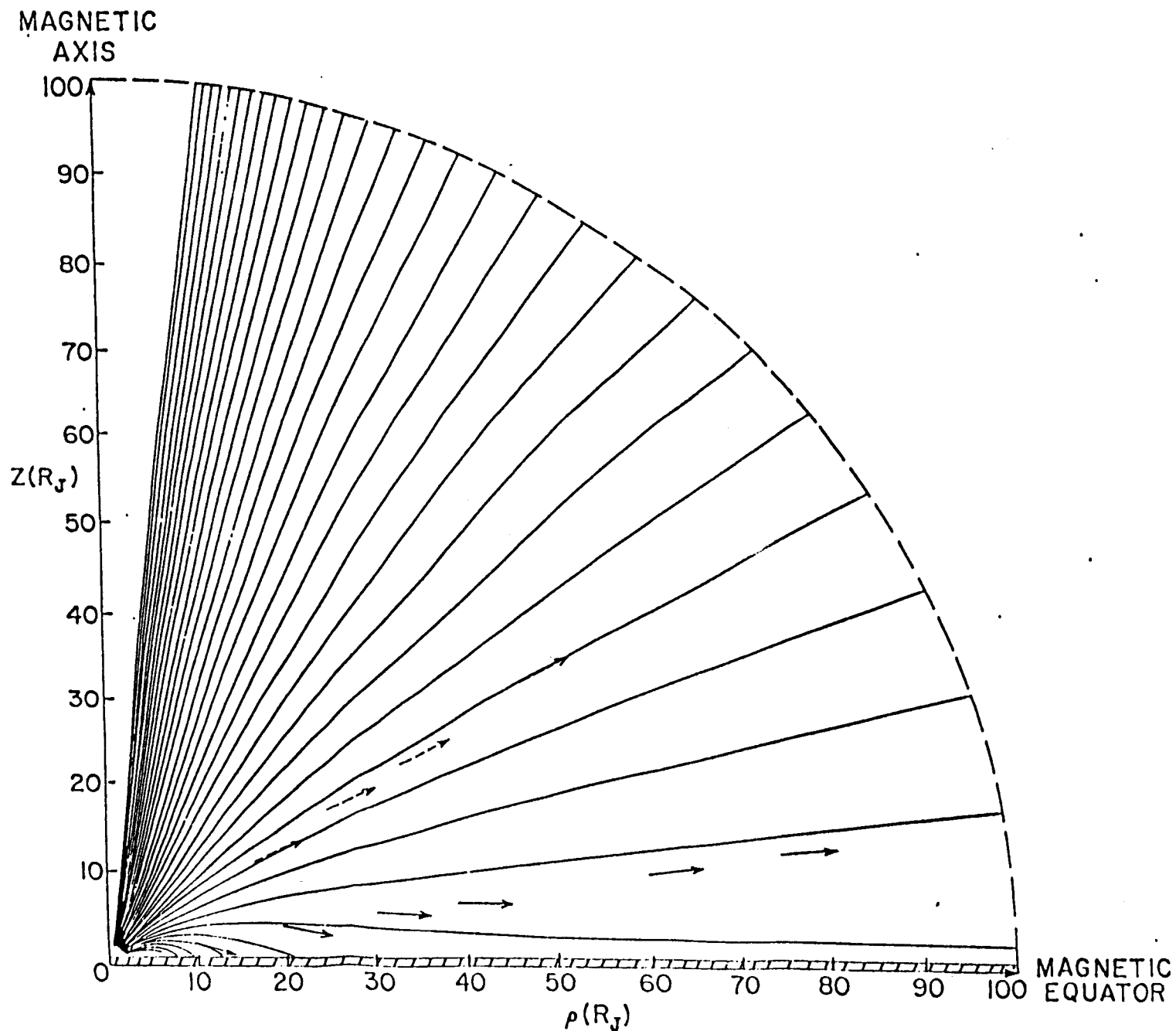


Figure 1: Plots of magnetic field lines for $f = -(AD/\rho^{a-1})(\ln \cosh z/D + 15)$; $g = \phi$

The first two sech^2 terms are disc currents, while the middle terms are volume currents concentrated near the symmetry axis, - as is the last term. Because $a \approx 0.7$, both the J_ϕ and J_z currents tend to ∞ as $\rho \rightarrow 0$. Hence, outside the data fitting region the corresponding magnetic field lines cannot be expected to represent the Jovian magnetosphere. The Euler potential model described in Jones et al. (1980), provides a better rms fit of 2.2 nT, but problems with non-physical fields and currents near the origin still exist.

The Khurana Model

The Khurana Euler potentials f and g and their partials are given in the Appendix 1 (from Khurana, 1997). We have simplified the functions by removing any ϕ dependence and setting Z_{cs} and its derivatives = 0. In this representation the singularity in f at $r (= \sqrt{\rho^2+z^2}) = 0$, -otherwise present in the expressions of Goertz et al., (1976) and Jones and Melville (1975), -is removed and results in a marked improvement in the large scale nature of the global field pattern near the planet. This was achieved in part by introducing multiplicative hyperbolic functions of the argument (r_{01}/r) , i.e., $[\tanh(r_{01}/r)]^{a_1}$ and $[\text{sech}^2(r_{01}/r)]$. With $r_{01} \approx 40$ RJ and $a_1 \approx 3$, these functions are respectively 1 and 0 at $r = 0$, and respectively 0 and 1 for $r \rightarrow \infty$, and both are approximately 0.4 at $r = r_{01}$. However, for $z \neq 0$ along the symmetry axis, $r = 0$ is not achieved, and any portion of the field function that tends to ∞ as $\rho \rightarrow 0$ is not excluded. For small ρ and arbitrary z the magnetic field components are given by (see Appendix 2):

$$B_\rho = - (C_1 a_1 r_{01}/z^2) [\tanh(r_{01}/z)]^{(a_1-1)} [\text{sech}^2(r_{01}/z)] [\ln \cosh(z/D_1)] \\ + (C_1/D_1) [\tanh(r_{01}/z)]^{a_1} [\tanh(z/D_1)]$$

$$B_\phi = 0$$

$$B_z = - (C_1/\rho) [\tanh(r_{01}/z)]^{a_1} [\ln \cosh(z/D_1)] + (C_2 + C_3 + C_4)$$

The only component clearly anomalous for $\rho \rightarrow 0$ is B_z , which is plotted in Figure 2. Very near $\rho = 0$, B_z is positive for $z = 0$, but for other values of z it tends to negative infinity. Also, reasonably near (but not too close to) the symmetry axis and large z , B_z will be determined primarily by the constants $C_2, C_3, + C_4$, a clearly anomalous result.

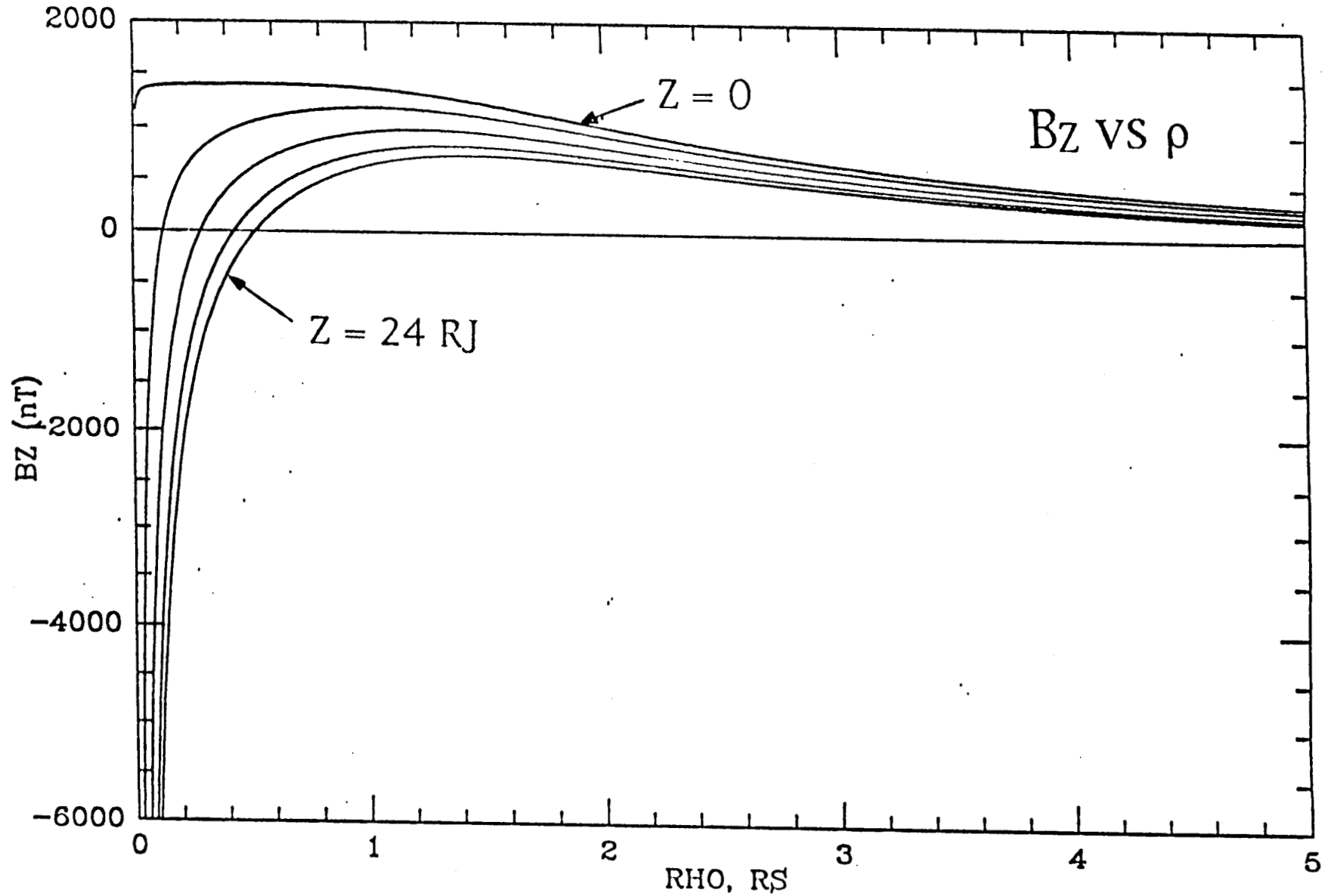


Figure 2: Plots of the Khurana Euler potential B_z component near the symmetry axis (i.e, for small ρ) for $z = 0$ (top curve), $z = 6 \text{ RJ}$, 12 RJ , 18 RJ , and 24 RJ (bottom curve)

The thin disc currents are (see Appendix 2):

$$\mu_0 J_\rho = p(C_1 \rho / D_1^2) [\tanh(r_{01}/r)]^{a_1} [\operatorname{sech}^2(z/D_1)]$$

$$\mu_0 J_{\phi 1} = [C_1 / (D_1^2)] [\tanh(r_{01}/r)]^{a_1} [\operatorname{sech}^2(z/D_1)]$$

The corresponding volume current densities in the vicinity of small ρ are:

$$\mu_0 J_\rho \approx 0 \text{ (all terms have } \rho \text{ multipliers)}$$

$$\begin{aligned} \mu_0 J_\phi \approx & [C_1 / D_1^2] [\tanh(r_{01}/r)]^{a_1} [\operatorname{sech}^2(z/D_1)] \\ & - (2C_1 / \rho^2) [\tanh(r_{01}/r)]^{a_1} [\operatorname{Incosh}(z/D_1)] \\ & + (C_1 / \rho D_1) [\tanh(r_{01}/r)]^{a_1} [\tanh(z/D_1)] \\ & + C_2 a_2 \rho_{02} / \rho^2 [\tanh(\rho_{02}/\rho)]^{a_2-1} [\operatorname{sech}^2(\rho_{02}/\rho)] \\ & + C_3 a_3 \rho_{03} / \rho^2 [\tanh(\rho_{03}/\rho)]^{a_3-1} [\operatorname{sech}^2(\rho_{03}/\rho)] \end{aligned}$$

$$\begin{aligned} \mu_0 J_z \approx & (C_1 a_1 r_{01} / r^3) [\tanh(r_{01}/r)]^{(a_1-1)} [\operatorname{sech}^2(r_{01}/r)] [\operatorname{Incosh}(z/D_1)] \\ & - C_1 / D_1 [\tanh(r_{01}/r)]^{a_1} [\tanh(z/D_1)] \end{aligned}$$

Thus, for $\rho \Rightarrow 0$ and arbitrary z , J_ρ goes to zero, J_z is well behaved and has primarily a functional dependence on z , and J_ϕ consists of the major disc current term plus several terms that approach ∞ as $1/\rho$ and $1/\rho^2$. In addition, the C_2 and C_3 terms show no dependence on z and thus will dominate at moderately small ρ and large z as expected based upon the behavior of B_z displayed in Figure 2.

The most troublesome current for $z \neq 0$, however, is the combination

$$\begin{aligned} \mu_0 J_\phi = & - (2C_1 / \rho^2) [\tanh(r_{01}/r)]^{a_1} [\operatorname{Incosh}(z/D_1)] \\ & + C_2 a_2 \rho_{02} / \rho^2 [\tanh(\rho_{02}/\rho)]^{a_2-1} [\operatorname{sech}^2(\rho_{02}/\rho)] \\ & + C_3 a_3 \rho_{03} / \rho^2 [\tanh(\rho_{03}/\rho)]^{a_3-1} [\operatorname{sech}^2(\rho_{03}/\rho)] \end{aligned}$$

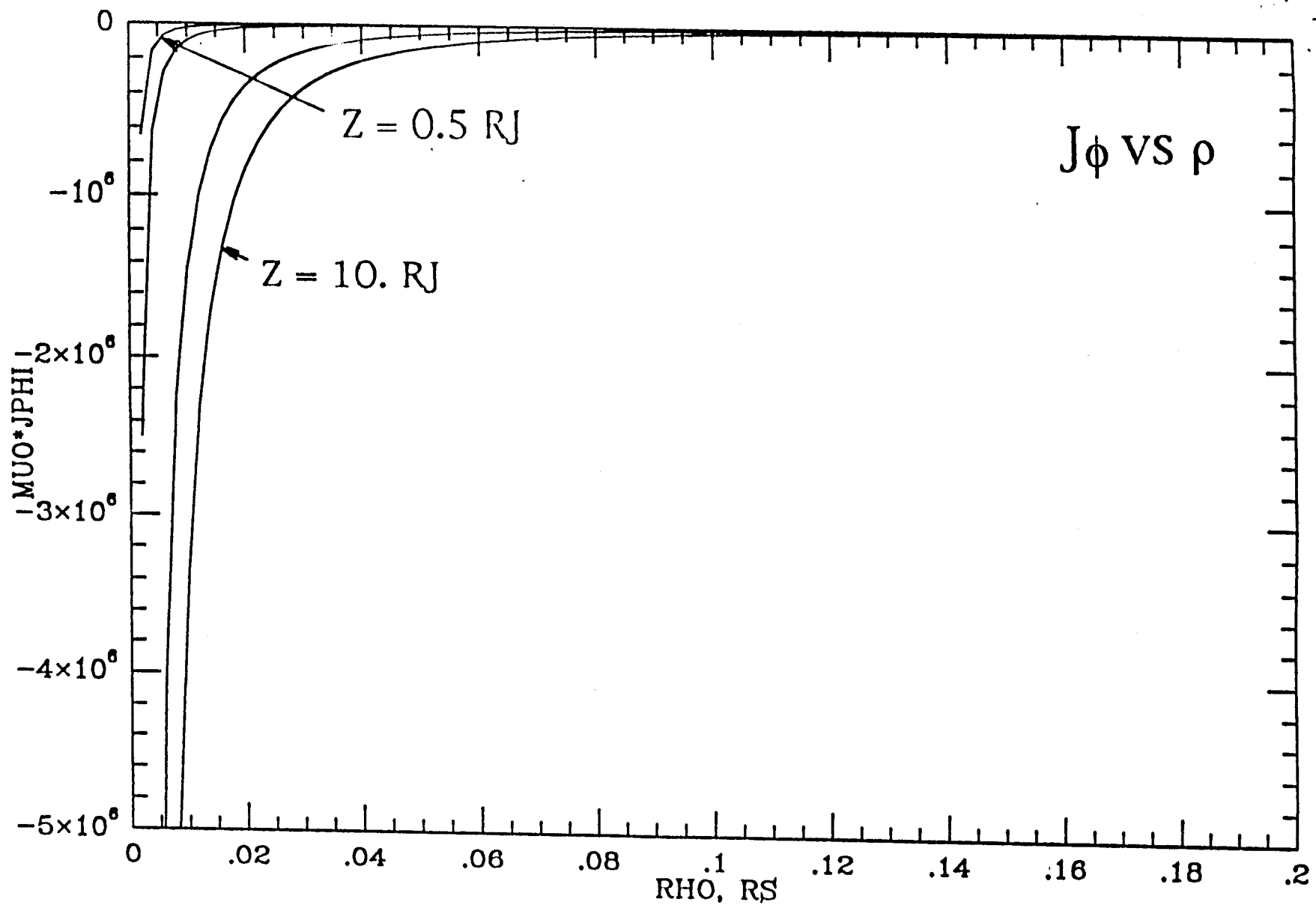


Figure 3: Plots of the Khurana Euler potential J_ϕ current component near the symmetry axis (i.e, for small ρ) for $z = 0.5 R_J$ (top curve), $z = 1.0 R_J$, $5.0 R_J$, and $10 R_J$ (bottom curve)

Figure 3 displays the manner in which the first term goes to $-\infty$ at $\rho = 0$ for any $z \neq 0$. Because of the dipole tilt of about 9.5° this alone would make the model unusable within a double conical volume having a full angular width a about 19° centered on the planetary spin axis.

A more serious problem is associated with the current in the next two terms, since they extend to $\pm \infty$. The $J_{\phi, \text{disc}}$ and total $J_{\phi, \text{volume}}$ currents are displayed in Figure 4 for comparison. One sees that for all z values, $J_{\phi, \text{volume}} \Rightarrow -\infty$ as $\rho \Rightarrow 0$ for $z \neq 0$. But in addition, there are $J_{\phi, \text{volume}}$ terms that are seen to dominate at ($\rho \approx$ a few RJ, large z). We have computed the total $J_{\phi, \text{volume}}$ current over ρ at each z increment through $z = \pm 50$ RJ and estimate it to be nearly 20 times the total current contained in the $J_{\phi, \text{disc}}$. Hence, even though one excludes the $\approx 19^\circ$ conical volume about the planetary spin axis where $J_{\phi, \text{volume}} \Rightarrow -\infty$, a major source of error in \mathbf{B} still remains when very far from the current disc.

Throughout much of the magnetosphere there are other currents required by this model that clearly cannot be physical. Referring to the complete expressions for \mathbf{J} given in Appendix 2, one notes that in addition to the J_ϕ terms discussed above, there are other "volume" currents of argument (z/D_1) of the form $\ln \cosh(z/D_1)$ and $\tanh(z/D_1)$ (the latter reverses across $z = 0$). These J_ρ and J_z volume currents are spatially modulated or "shaped" by (ρ, z) polynomial functions, hyperbolic functions with (r_{01}/r) arguments ($r_{01} \approx 40$ RJ), and hyperbolic functions with argument (z/D_2) ($\langle D_2 \rangle \approx 20$ RJ). The nature of the shaping of the ($\ln \cosh z/D_1$, $\tanh z/D_1$) volume currents terms produces, in turn, volume and several types of thick disc currents. Neglecting the shaping effects due to the (ρ, z) polynomial functions and hyperbolic functions with (r_{01}/r), the basic features may be characterized as follows:

$\ln \cosh z/D_1$ times $\tanh^2 z/D_2 \approx$ volume current with equatorial gap (half amplitude full width $\approx 2 \times 16$ RJ = 32 RJ) (curve 1)

$\ln \cosh z/D_1$ times $\tanh z/D_2$ $\text{sech}^2 z/D_2 \approx \pm$ current sheet/disc doublet (opposite polarity), peaks at $\approx \pm 13$ RJ (curve 2)

$\ln \cosh z/D_1$ times $\tanh^2 z/D_2$ $\text{sech}^2 z/D_2 \approx$ current sheet/disc doublet (same polarity), peaks at $\approx \pm 18$ RJ (curve 3)

$\ln \cosh z/D_1$ times $\text{sech}^4 z/D_2 \approx$ thick current sheet/disc at equator (full half amplitude width $\approx 2 \times 10$ RJ = 20 RJ) (curve 4)

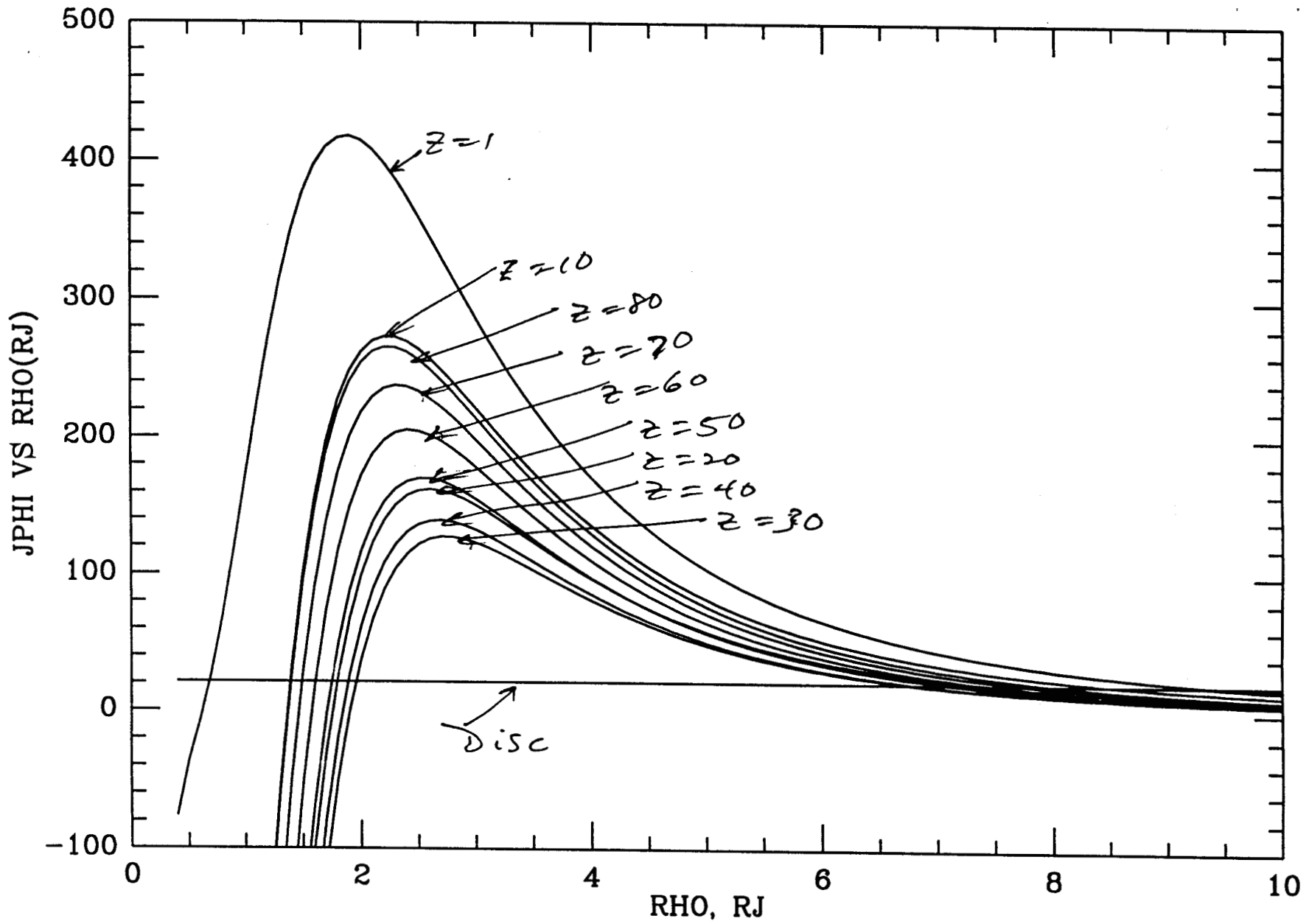


Figure 4

with similar expressions using $\tanh(z/D_1)$. The above modulated functions are displayed in Figures 5 ($\ln \cosh z/D_1$) and 6 ($\tanh z/D_1$). For purposes of orientation, the $\text{sech}^2(z/D_1)$ thin disc function is also plotted (central narrow peak). For completeness we display in Figure 7 the (r_0/r) hyperbolic shaping functions $[\tanh(r_0/r)]^{a_1}$, $[\tanh(r_0/r)]^{a_1}[\text{sech}^2(r_0/r)]$ and $[\tanh(r_0/r)]^{a_1-1}[\text{sech}^2(r_0/r)]$.

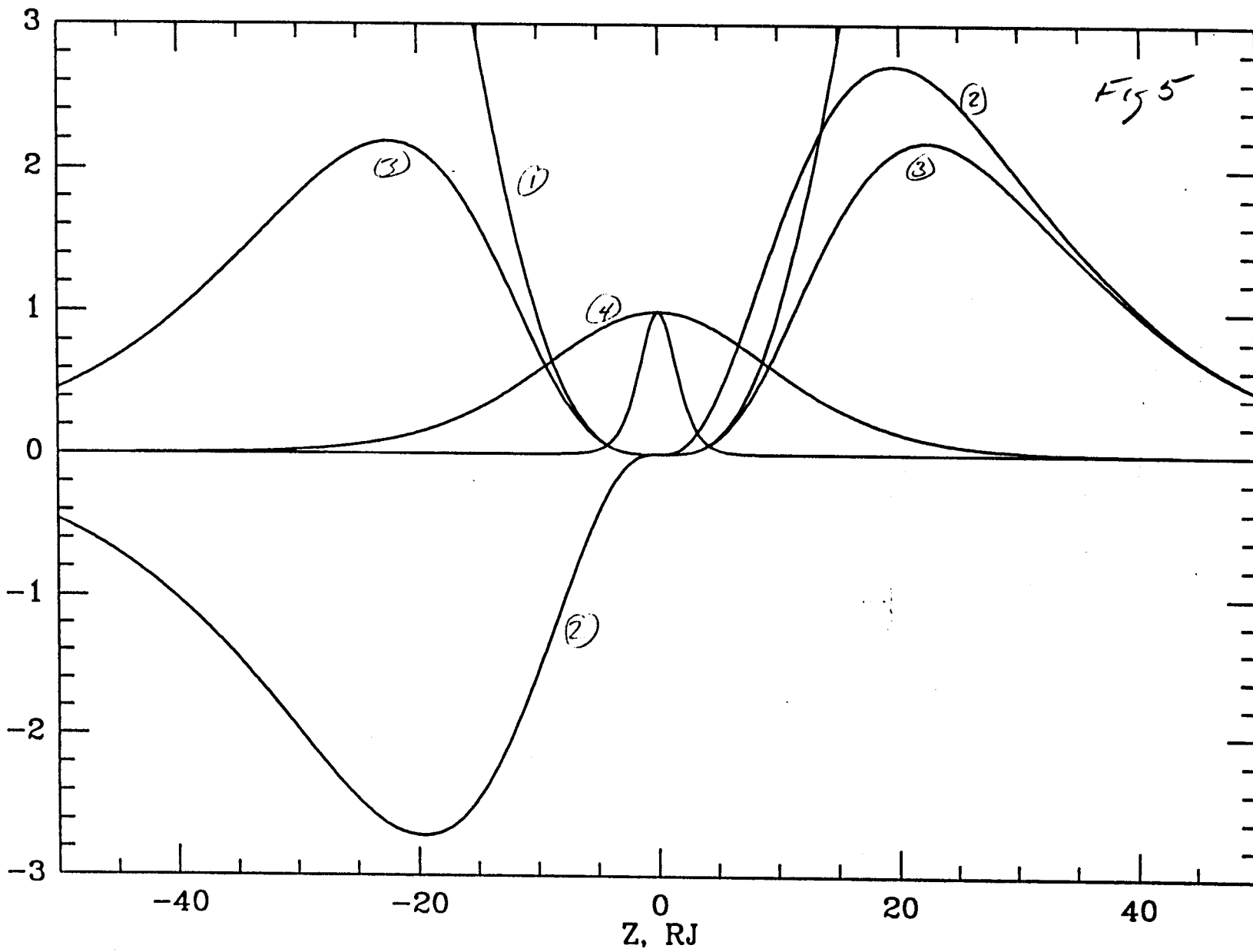
Although the J_ρ and J_z currents are relatively small, amounting to several percent of that in the azimuthal disc current, the volume over which they act is large and their effect on the nature of \mathbf{B} far from the disc cannot be neglected. Hence, considering all of the model currents we conclude that none of the Euler potential models based upon the Harris current sheet can be used to infer the global nature of the magnetic field of Jupiter. Its primary value, then, is in its ability to infer the nature and shape of the current disc.

Global Configuration of the Khurana Model

Figures 8 and 9 display a number of magnetic field lines that result when the Khurana (1997) Euler potential model is combined with the O6 planetary magnetic field model of Connerney (1993). The (r, ϕ, θ) starting points for each of the lines are indicated in the figures. The primary contribution of the Khurana sheet terms is to make some of the lines depart from a pure planetary source form. This is seen in the straying of the field lines northward parallel to the z -axis, although there are problems with a few of the lines extending from near the south polar axis. These problems can be explained if there is a region about the symmetry axis of the planetary dipole in which the z component of the magnetic field tends to parallelism with that symmetry axis. The absence of a simple cusp region is obvious. The anomalous character of the high latitude lines may also be due to the presence of the non-physical J_ϕ volume currents discussed previously. Such problems with the field lines do not occur when the O6 planetary field model and "plumber-washer corotating current disk" (Connerney, 1993) are combined.

Figures 10 and 11 display the field line configuration resulting when the Khurana model magnetic field is combined with the "idealized" magnetopause field due to the solar wind interaction (Engle, 1991). Figure 10 shows a few sample lines, all of which have their starting locations labeled. Figure 11 has the x - z plane projections of the entire family of lines originating from the planet surface near the south pole in the noon or midnight meridian plane. In that study the planetary field was a planet-

(Z/D2) FUNCTION MODULATION OF LN COSH(Z/D1) VS Z(RJ)



(Z/D2) FUNCTION MODULATION OF TANH(Z/D1) VS Z(RJ)

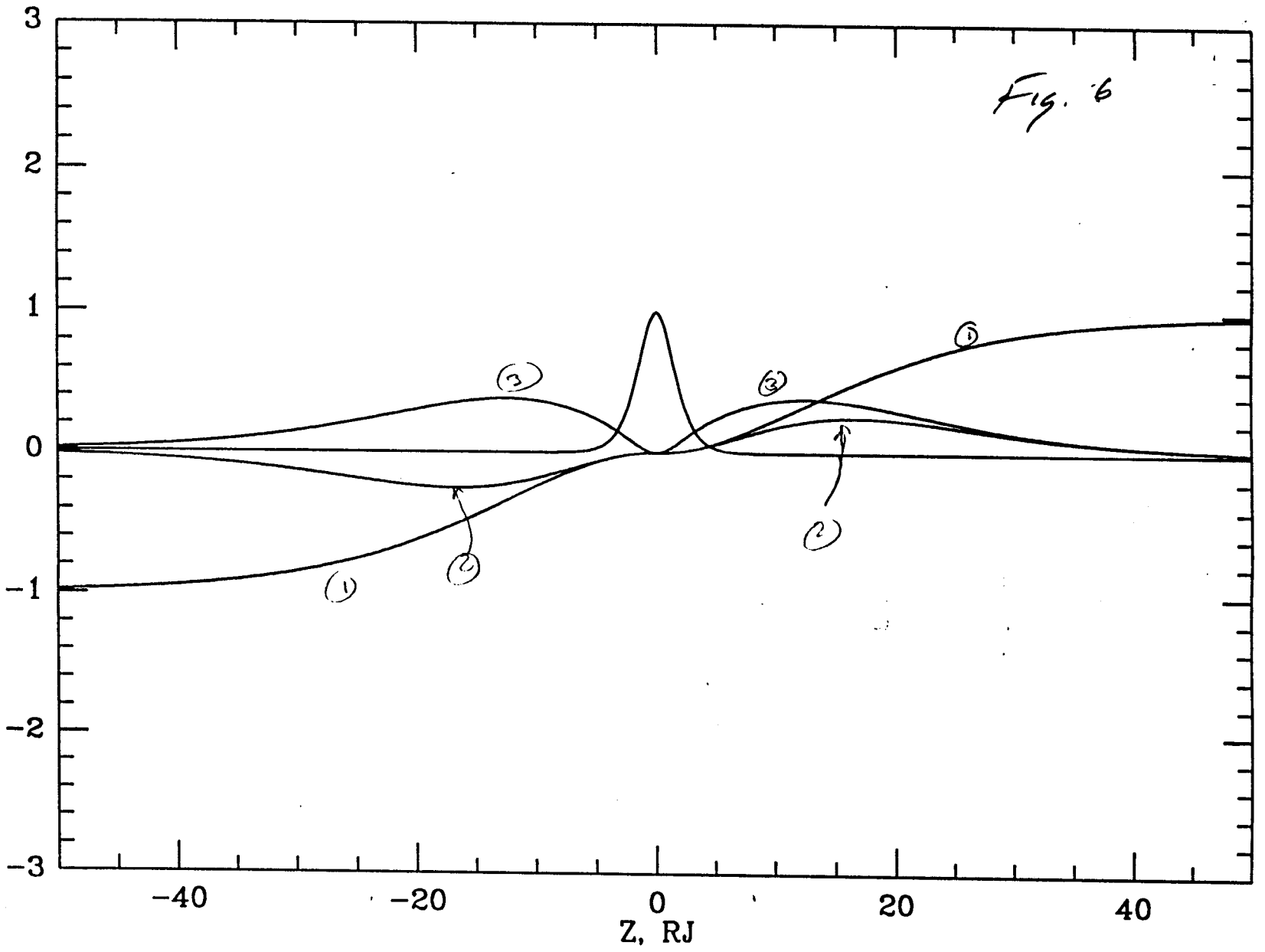


Fig. 6

HYPERBOLIC (R01/R) SHAPE FUNCTION

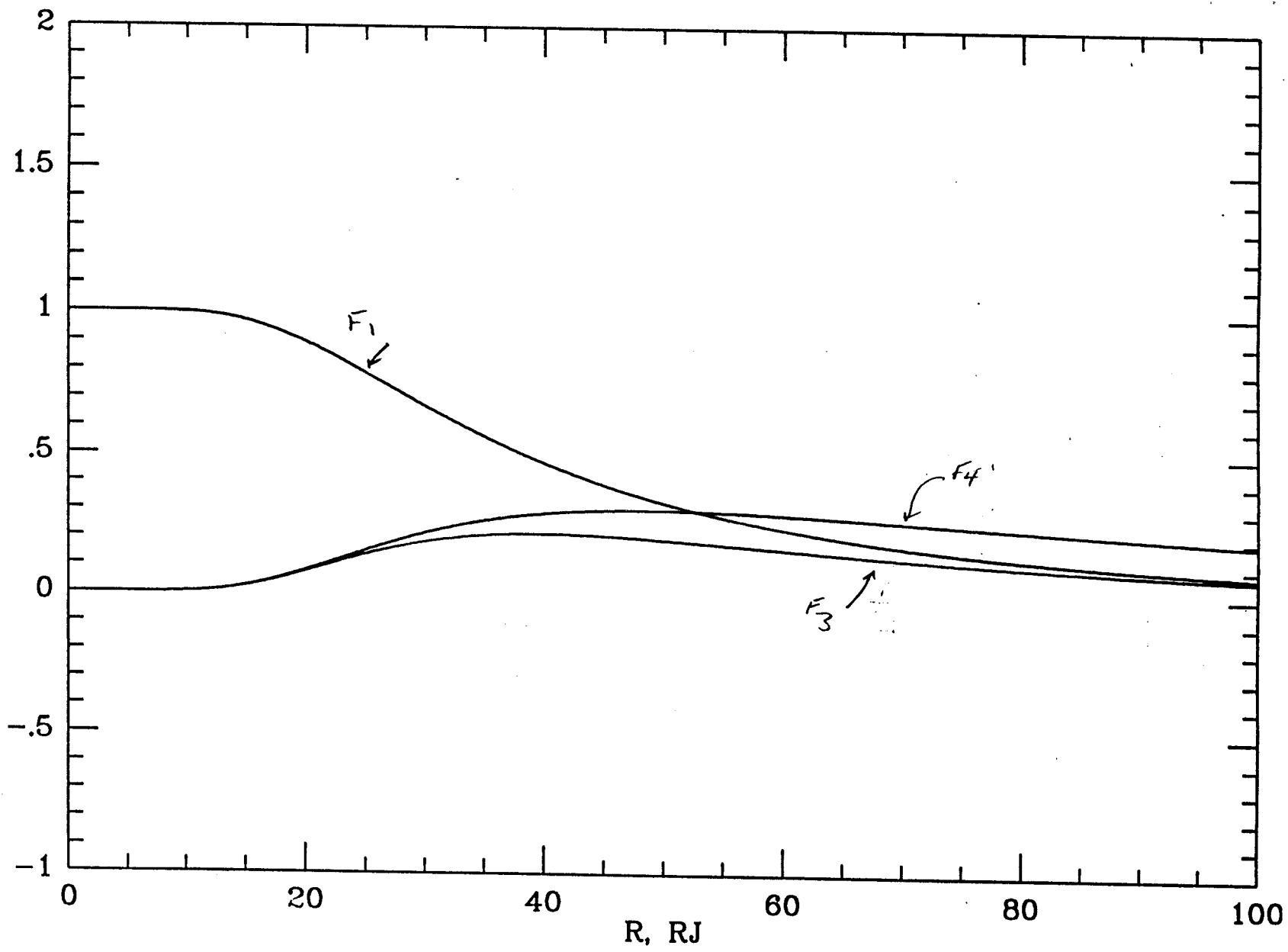


Fig 7

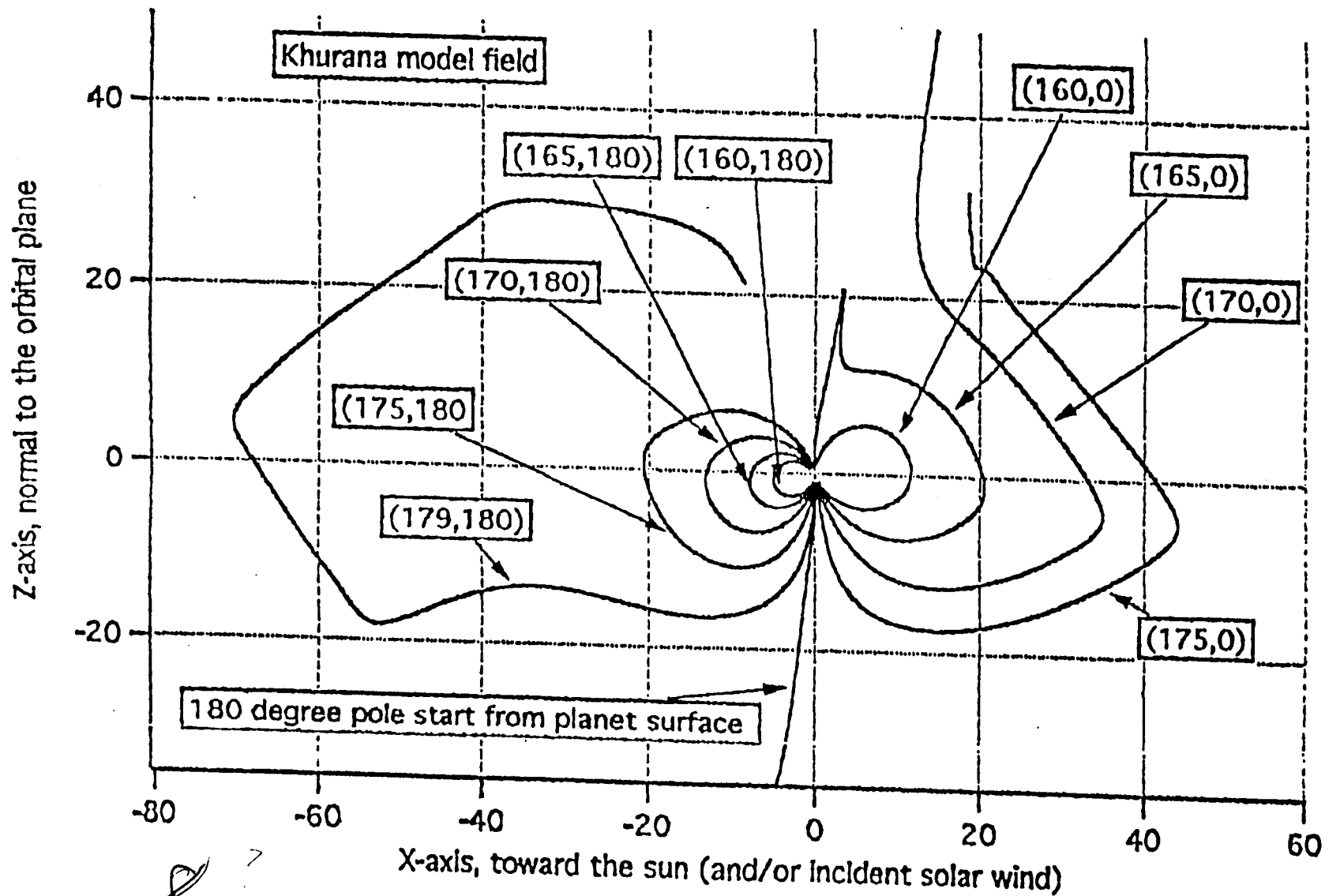


Figure 4: Magnetic field lines obtained using the Khurana disc magnetic field model developed using Euler potentials, combined with the O6 planetary field model of Connerney et al. (1992). A (θ, ϕ) line notation is used, where ϕ is either 0° (noon) or 180° (midnight). Notice the difficulty with the model field lines in the vicinity of the symmetry axis.

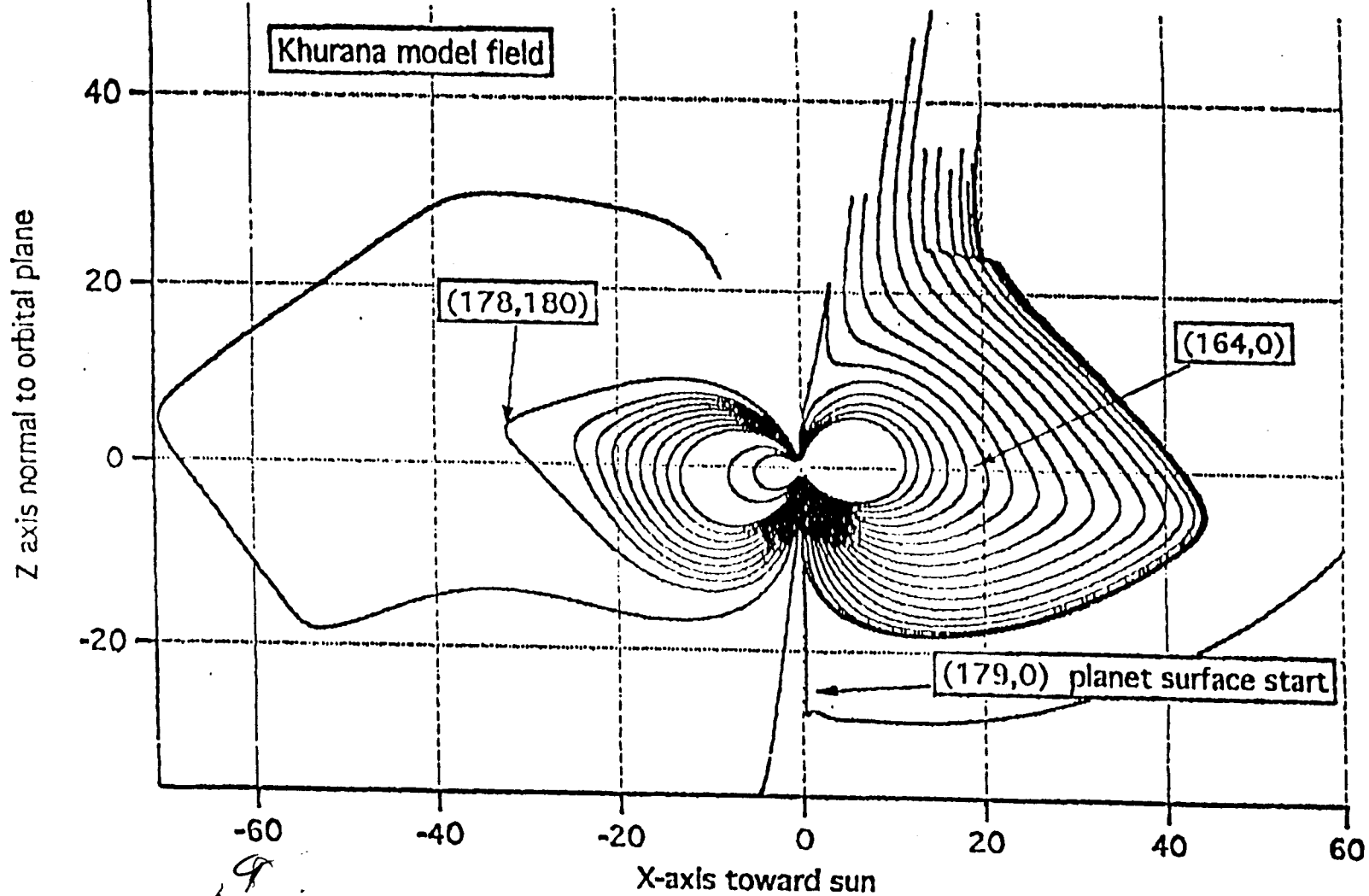


Figure 5: X-Z plane projections of the entire family of lines originating from the planet surface near the south pole in the noon or midnight meridian for the model configuration outlined in Figure 4 above. The model not only fails in the immediate vicinity of the polar regions, but these plots suggest that the model also requires unphysical volume currents well outside the fitting region,- a characteristic found in earlier attempts to model the Jovian magnetosphere using Euler potentials (Jones and Melville, 1975).

Fig 10

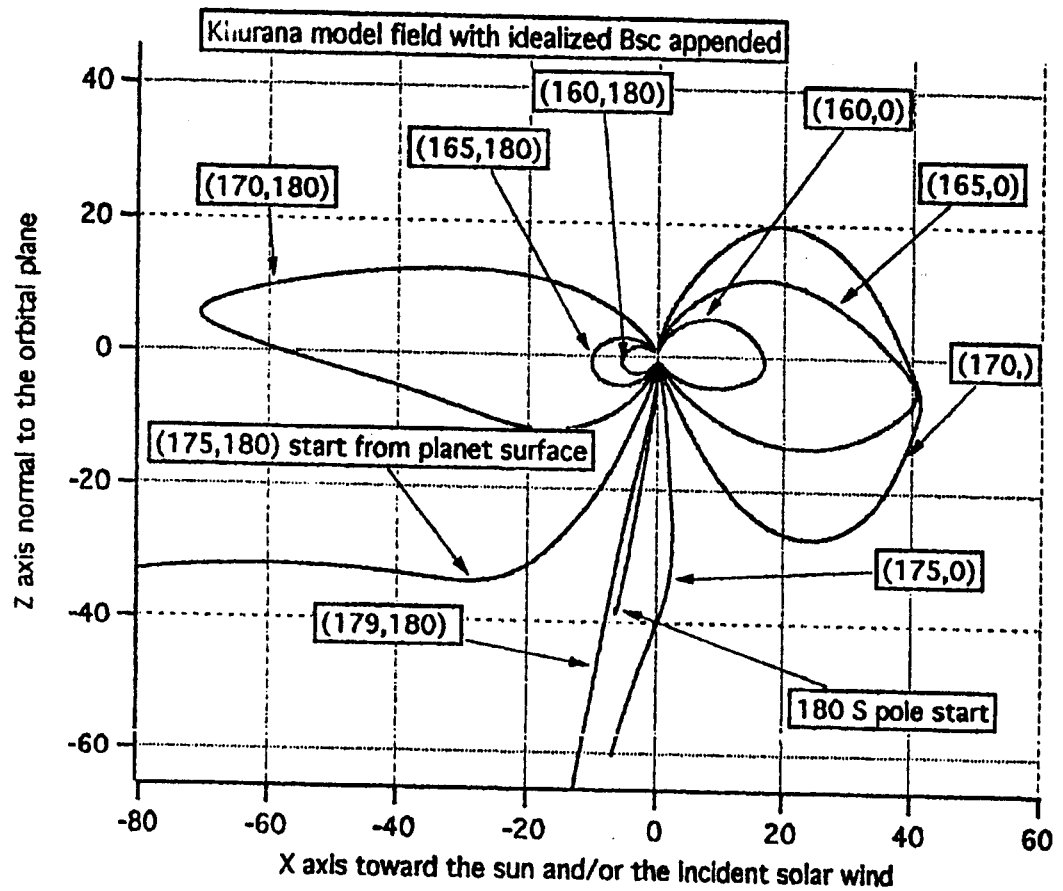
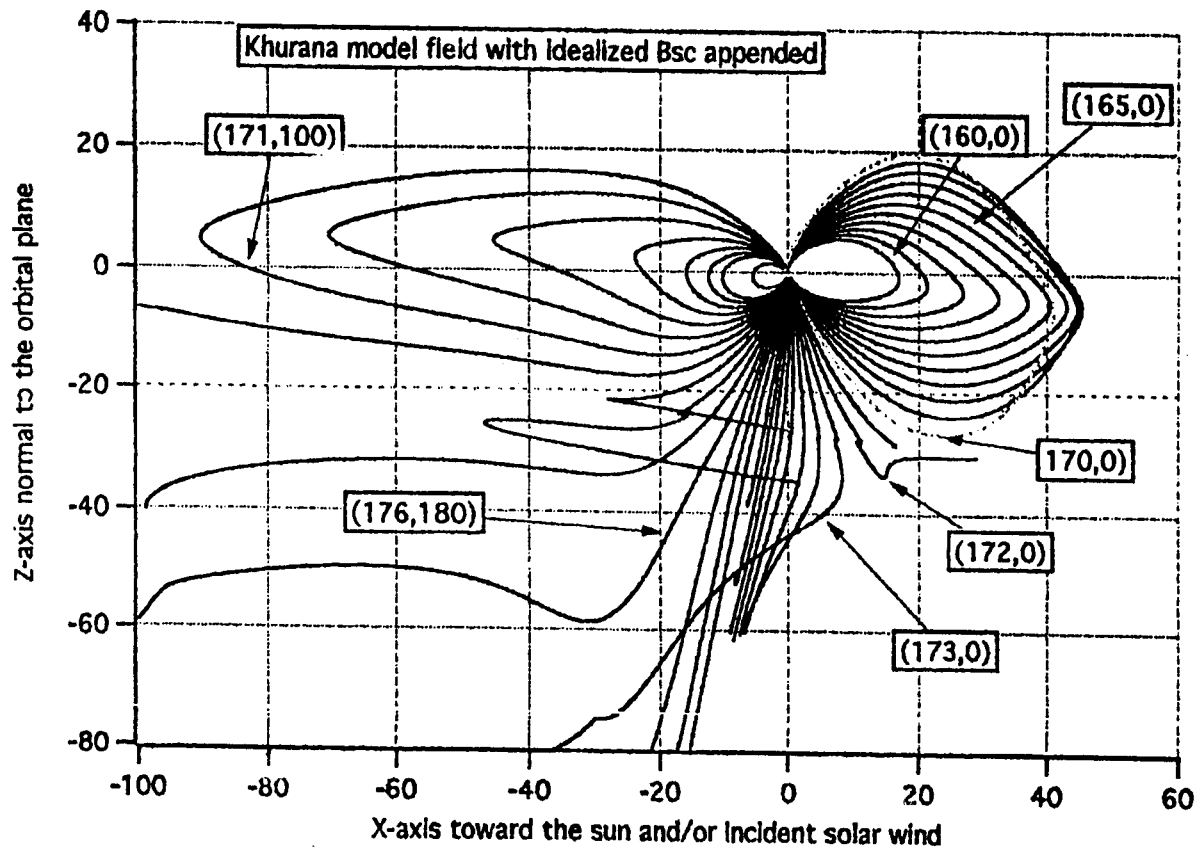


Fig 11



centered dipole, whereas in this study, the O6 model is used for the planetary field. Although looking somewhat well behaved, there are, -as before, - some lines which are simply ill-behaved. They are primarily in a cone near the south pole (177,180), (178,180), (179,180), (180,180), but also there are 2 peculiar lines originating at (173,180) and (174,180), even though the two lines originating at (176,180) and (175,180) seem to be reasonably well-behaved tail lines.

Discussion and Conclusions

Goertz et al. (1974), Jones and Melville (1975), Goertz et al. (1976) and Jones et al. (1980) used cylindrical coordinate forms of a Harris current sheet type of Euler function to model Jupiter's magnetosphere over the relatively small portion explored by the outbound Pioneer 10 (equatorial dawn line). The common thread in these various studies was the application of the method to estimate the basic nature of the giant Jovian current disc, and to infer some of the trends of the field in the nearby region; i.e., the suggestion of open field lines near the dawn meridian (Goertz et al., 1976). In each case the non-physical nature of the field resulting from non-physical currents, -principally tending to ∞ near the origin, etc., -was realized and appropriate constraints placed on the discussion. Thus, the use of the Harris type hyperbolic functions, - although fairly straightforward in terms of manipulation and fitting of restricted data regions, - appeared to be limited because of their behaviour near the planet, particularly along the symmetry axis. Several discussions regarding the problems with this basic form of Euler potential in terms of global application were presented (Jones and Melville, 1975; Jones et al., 1980) and in the case of the latter study the focus was shifted towards a current modeling disc method in which bounded currents were established as part of the model (Jones et al., 1980; Thomas and Jones, 1984; Jones et al., 1993)

By using more complex forms for the Harris sheet derived Euler potentials f and g , Khurana (1997) has been able to obtain good fits to the Pioneer 10, Voyager 1 and 2 outbound data, and to describe more completely the distortions of the Jovian current disc. However, we find that the particular type of Euler functions used in the model produce two strong solenoidal currents, both of which are essentially unconstrained in z ; a thin infinite solenoidal current aligned with the symmetry axis, and a thicker, finite solenoidal current of opposite sign also aligned with the symmetry axis. The total current in the thick, finite solenoid is considerably greater (≈ 20 times) than the total in the physical disc current. Also, there are a number of other non-physical volume and thick

disc currents that can cause globally significant magnetic field effects. As a result, the model is of little value for any global type magnetic field studies (solar wind pressure balance determination of the magnetopause shape, location of the cusp, trapped particle and auroral foot print studies, etc.).

We conclude that hyperbolic Euler potentials are of questionable value for global modeling of a planetary magnetosphere that is dominated by a strong current disc like Jupiter. However, other types of potentials have been used to successfully model the terrestrial magnetosphere, a magnetosphere in which internal currents play a minor role (Chen, 1995). Thus, one cannot exclude, in general, the use of Euler potentials for Jovian magnetosphere modelling.

However, we should also note that a study of both the inbound and outbound data sets from Pioneers 10 and 11 has shown that B_ϕ depends upon local time, it being a maximum along the dawn meridian and tending to near zero along the noon meridian (Jones et al., 1981). This observed local time dependence of B_ϕ has been attributed to the possible existence of a dayside tail-like current sheet (Jones et al., 1981; Thomas and Jones, 1984). This has been supported by further studies of the Jovian magnetic field by the Ulysses spacecraft which have suggested that the B_ϕ pattern is symmetric about the noon meridian, i.e., that there is therefore strong tailward draping of the magnetic field (Jones et al., 1993; Jones et al., 1995). Thus, the nature of the equatorial currents at Jupiter may be far more complicated than originally considered. Modeling of such a magnetosphere in terms of Euler potentials clearly requires a major change in the nature of the function, since the present coefficients would need to display a local time dependence. It would therefore seem unlikely that the true nature of the Jovian equatorial currents can be obtained using this modeling approach.

References

Engle, I. M., Jovian Magnetosphere, Including the Dayside Solar Wind Interaction and the Khurana Jovian Floppy Magnetodisk, Paper presented at the conference Magnetospheres of the Outer Planets held at the University of Colorado, Boulder, Colorado, March 17-21, 1997.

Cheng, C. Z., Three-dimensional Magnetic Equilibrium with Isotropic Pressure, Geophys. Res. Lett., 22, 2401-2404, 1995.

Connerney, J. E. P., Magnetic Fields of the Outer Planets, J. Geophys. Res., 98, 18659, 1993.

Engle, I. M., Idealized Voyager Jovian Magnetosphere Shape and Field, J. Geophys. Res., 96, 7793-7802, 1991.

Engle, I. M., Jovian Magnetosphere, Including the Dayside Solar Wind Interaction and the Khurana Magnetotail, Paper presented at the Conference Magnetospheres of the Outer Planets held at the University of Colorado, Boulder, Colorado, March 17-21, 1997.

Goertz, C. K., B. A. Randall, and M. F. Thomsen, A model for the Jovian Magnetic Field, EOS, 55, 1172, 1974 (paper presented at the Fall 1974 meeting of the American Geophysical Union, Dec. 12-17, 1974]).

Goertz, C. K., D. E. Jones, B. A. Randall, E. J. Smith, and M. F. Thomsen, Evidence for Open Field Lines in Jupiter's Magnetosphere, J. Geophys. Res., 81, 3393-3398, 1976.

Jones, D. E., and J. G. Melville, Preliminary Model Studies of the Magnetosphere of Jupiter: Pioneer 10, Proc. Utah Acad. Sci., Arts., Letters, 52, 14-27, 1975.

Jones, D. E., J. G. Melville, and M. L. Blake, Modelling Jupiter's Current Disc: Pioneer 10 Outbound, J. Geophys. Res., 85, 3329-3336, 1980.

Jones, D. E., B. T. Thomas, and J. G. Melville II, Equatorial Disk and Dawn-Dusk Currents in the Frontside Magnetosphere of Jupiter: Pioneers 10 and 11, J. Geophys. Res., 86, 1601-1605, 1981.

Jones, D. E., E. J. Smith, N. Murphy, D. Winterhalter, A. Balogh, and D. J. Southwood, A Model of Jovian Magnetospheric Current System Based Upon Magnetic Field Data Obtained by the Ulysses Helium Vector Magnetometer, EOS, 74, 529, 1993 (abstract of paper presented at the Fall Meeting of the AGU, San Francisco, December 1993).

Jones, D. E., L. Gordon and C. J. Alexander, Predictions of the Magnetic Field of Jupiter Along Several Representative Orbits of the Galileo Spacecraft Based Upon Model fits Derived From Pioneer and Ulysses Magnetic Field Data, EOS, 76, 346, 1995 (abstract of paper presented at the Fall Meeting of the AGU, San Francisco, December 1995).

Khurana, K. K., Euler Potential Models of Jupiter's Magnetospheric Field, J. Geophys. Res., 102, 11295-11306, 1997.

Thomas, B. T., and D. E. Jones, Modeling of Jupiter's Magnetospheric Currents Using Pioneer Data: Evidence for a Low-latitude Cusp, J. Geophys. Res., 89, 6663-6670, 1984.

Appendix 1 : The KKK Euler Potentials

For simplicity in this study we have removed any ϕ dependence from the Euler potential expressions given by Khurana (1997) and set $Z_{cs} = 0$. Thus, for this study, the f and g functions and their partials are:

$$f = - C_1 \rho [\tanh(r_{01}/r)]^{a_1} \ln \cosh(z/D_1)$$

$$\int \rho \{ C_2 [\tanh(\rho_{02}/\rho)]^{a_2} + C_3 [\tanh(\rho_{03}/\rho)]^{a_3} + C_4 \} d\rho$$

$$g = \phi + p(1+q \tanh^2 z/D_2)\rho$$

Thus,

$$\begin{aligned} \partial f / \partial \rho = & -C_1 [\tanh(r_{01}/r)]^{a_1} \ln \cosh(z/D_1) + \\ & C_1 a_1 r_{01} \rho^2 / r^3 [\tanh(r_{01}/r)]^{a_1-1} [\operatorname{sech}(r_{01}/r)]^2 \ln(\cosh(z/D_1)) + \\ & C_2 \rho [\tanh(\rho_{02}/\rho)]^{a_2} + C_3 \rho [\tanh(\rho_{03}/\rho)]^{a_3} + C_4 \rho \end{aligned}$$

$$\partial f / \partial \phi = 0$$

$$\begin{aligned} \partial f / \partial z = & C_1 a_1 r_{01} (\rho z / r^3) [\tanh(r_{01}/r)]^{a_1-1} [\operatorname{sech}(r_{01}/r)]^2 \ln[\cosh(z/D_1)] \\ & - C_1 \rho / D_1 [\tanh(r_{01}/r)]^{a_1} \tanh(z/D_1) \end{aligned}$$

$$\partial g / \partial \rho = p \{ 1 + q [\tanh(z/D_2)]^2 \}$$

$$\partial g / \partial \phi = 1$$

$$\partial g / \partial z = (2pq/D_2)\rho \tanh(z/D_2) [\operatorname{sech}(z/D_2)]^2$$

The constants used in this study are those listed in Khurana (1997) Table 1, for Pioneer 10 outbound, i.e.,

$C_1 = 70.2$	$a_2 = 2.06$
$C_2 = 1369.9 \text{ (RJ)}^{-1}$	$a_3 = 7.55$
$C_3 = 33.4 \text{ (RJ)}^{-1}$	$\rho_{02} = 2.55 \text{ RJ}$
$C_4 = -1.1$	$\rho_{03} = 32.8 \text{ RJ}$
$D_1 = 1.83 \text{ RJ}$	$r_{01} = 44.1 \text{ RJ}$
$D_2 = 20.60 \text{ RJ}$	$p = 6.66 \times 10^{-3}$
$a_1 = 3.27$	$q = 0.32$

Appendix 2: The KKK Fields and Currents

The field equations (with Z_{cs} and its derivatives = 0) are

$$B_\rho = -(C_1 a_1 r_{01} z / r^3) [\tanh(r_{01}/r)]^{a_1-1} [\text{sech}^2(r_{01}/r)] [\ln \cosh(z/D_1)] \\ + (C_1/D_1) [\tanh(r_{01}/r)]^{a_1} [\tanh(z/D_1)]$$

$$B_\phi = \{ (C_1 a_1 r_{01} \rho z / r^3) [\tanh(r_{01}/r)]^{a_1} [\text{sech}^2(r_{01}/r)] [\ln \cosh(z/D_1)] \\ - C_1 \rho / D_1 [\tanh(r_{01}/r)]^{a_1} \tanh(z/D_1) \} \{ p(1+q[\tanh^2(z/D_2)]) \} \\ + \{ C_1 [\tanh(r_{01}/r)]^{a_1} [\ln \cosh(z/D_1)] \\ - [C_1 a_1 r_{01} \rho^2 / r^3] [\tanh(r_{01}/r)]^{a_1-1} [\text{sech}^2(r_{01}/r)] [\ln \cosh(z/D_1)] \\ - C_2 \rho [\tanh(\rho_{02}/\rho)]^{a_2} - C_3 \rho [\tanh(\rho_{03}/\rho)]^{a_3} - C_4 \rho \} \\ \{ (2pqp/D_2) [\tanh(z/D_2)] [\text{sech}^2(z/D_2)] \}$$

$$B_z = -(C_1/\rho) [\tanh(r_{01}/r)]^{a_1} [\ln \cosh(z/D_1)] \\ + (C_1 a_1 r_{01} \rho / r^3) [\tanh(r_{01}/r)]^{a_1} [\text{sech}^2(r_{01}/r)] [\ln \cosh(z/D_1)] \\ + C_2 [\tanh(\rho_{02}/\rho)]^{a_2} + C_3 [\tanh(\rho_{03}/\rho)]^{a_3} + C_4$$

With $z=0$ and ρ small

$$B_\rho^* \approx -(C_1 a_1 r_{01} z / r^3) [\tanh(r_{01}/r)]^{a_1-1} [\text{sech}^2(r_{01}/r)] [\ln \cosh(z/D_1)] \rightarrow 0 \text{ as} \\ z, \rho \rightarrow 0$$

$$B_\phi = 0$$

$$B_z = -(C_1/\rho)[\tanh(r_{01}/r)]^{a_1} [\ln \cosh(z/D_1)] + C_2 + C_3 + C_4$$

→ 0 as z, ρ → 0

For a more careful look at the Khurana model we need the complete expression for the currents. With the current given by $\mu_o \mathbf{J} = \nabla \times \mathbf{B}$, we have with the simplification $\partial/\partial\phi = 0$

$$\mu_o \mathbf{J} = -(\partial B_\phi/\partial z)\rho + (\partial B_\rho/\partial z - \partial B_z/\partial\rho)\phi + [(1/\rho)B_\phi + \partial B_\phi/\partial\rho]\mathbf{k}$$

Expressing the several forms of the hyperbolic functions of the argument (r_{01}/r) as multiplicative functions F1 to F5,- where

$$\begin{aligned} F1 &= [\tanh(r_{01}/r)]^{a_1} \\ F2 &= [\tanh(r_{01}/r)]^{a_1-1} \\ F3 &= [\tanh(r_{01}/r)]^{a_1} [\operatorname{sech}^2(r_{01}/r)] \\ F4 &= [\tanh(r_{01}/r)]^{a_1-1} [\operatorname{sech}^2(r_{01}/r)] \\ F5 &= [\tanh(r_{01}/r)]^{a_1-2} [\operatorname{sech}^4(r_{01}/r)],- \end{aligned}$$

times the three hyperbolic functions of (z/D_1) , i.e., $\ln \cosh(z/D_1)$ (volume current), $\tanh(z/D_1)$ (reversing volume current), and $\operatorname{sech}^2(z/D_1)$ (disc current), the complete expression for the current obtained from the expressions for \mathbf{B} can be written as:

$$\begin{aligned} \mu_o J_\rho = - \{ \{ & -[2C_1 a_1 r_{01}^2 \rho z^2 / r^6][F3] + [(C_1 a_1 r_{01} \rho / r^3)(1-3z^2/r^2)][F4] \\ & + [C_1 a_1 (a_1-1) r_{01}^2 \rho z^2 / r^6][F5] \} \{ \ln \cosh(z/D_1) \} \\ & + [2C_1 a_1 r_{01} \rho z / (D_1 r^3)][F4] [\tanh(z/D_1)] - (C_1 \rho / D_1^2)[F1][\operatorname{sech}^2(z/D_1)] \\ & \{ p(1+q[\tanh^2(z/D_2)]) \} \\ & - \{ [C_1 a_1 r_{01} \rho z / r^3][F4][\ln \cosh(z/D_1)] - (C_1 \rho / D_1)[F1] [\tanh(z/D_1)] \} \\ & \{ (2pq/D_2)[\tanh(z/D_2)][\operatorname{sech}^2(z/D_2)] \} \\ & - \{ \{ - [C_1 a_1 r_{01} z / r^3][F2] + [3C_1 a_1 r_{01} \rho^2 z / r^5][F4] + [C_1 a_1 (a_1-1) r_{01}^2 \rho^2 z / r^6][F5] \\ & + [2C_1 a_1 r_{01}^2 \rho^2 z / r^6][F3] \} \{ \ln \cosh(z/D_1) \} \\ & + \{ (C_1 / D_1)[F1] - [C_1 a_1 r_{01} \rho^2 / D_1 r^3][F4][\tanh(z/D_1)] \} \} \\ & \{ (2pq\rho/D_2)[\tanh(z/D_2)][\operatorname{sech}^2(z/D_2)] \} \end{aligned}$$

$$- \{ \{ C_1[F1] - C_1 a_1 r_{01} \rho^2 / r^3 \} [F4] \} [\ln \cosh(z/D_1)] \\ - C_2 \rho [\tanh(\rho_{02}/\rho)]^{a_2} - C_3 \rho [\tanh(\rho_{03}/\rho)]^{a_3} - C_4 \rho \} \\ \{ (2pq\rho/D_2^2) [\operatorname{sech}^4(z/D_2)] + (4pq\rho/D_2^2) [\tanh^2(z/D_2)] [\operatorname{sech}^2(z/D_2)] \} \}$$

$$\mu_0 J_{\phi 1} = \{ 2C_1 a_1 r_{01} z / r^4 \} [F4] + C_1 a_1 (a_1 - 1) r_{01}^2 z / r^5 \} [F5] \\ + 2C_1 a_1 r_{01}^2 z / r^5 \} [F3] \} [\ln \cosh(z/D_1)] \\ - [C_1 a_1 r_{01} / (D_1 r^2)] [1 + z/r] [F4] [\tanh(z/D_1)] \\ + [C_1 / (D_1^2)] [F1] [\operatorname{sech}^2(z/D_1)]$$

and

$$\mu_0 J_{\phi 2} = \{ - 2C_1 / \rho^2 \} [F1] - [C_1 a_1 r_{01} / r^3 \{ (3\rho^2 / r^2) - 1 \}] [F4] \\ + [C_1 a_1 (a_1 - 1) r_{01}^2 \rho^2 / r^6] [F5] + [2C_1 a_1 r_{01}^2 \rho^2 / r^6] [F3] \} [\ln \cosh(z/D_1)] \\ + \{ - [C_1 r_{01} / r^3] [a_1 + \rho / D_1] [F4] + [C_1 / \rho D_1] [F1] \} [\tanh(z/D_1)] \\ + C_2 a_2 \rho_{02} / \rho^2 [\tanh(\rho_{02}/\rho)]^{a_2 - 1} [\operatorname{sech}^2(\rho_{02}/\rho)] \\ + C_3 a_3 \rho_{03} / \rho^2 [\tanh(\rho_{03}/\rho)]^{a_3 - 1} [\operatorname{sech}^2(\rho_{03}/\rho)]$$

And finally, for the z current, J_z

$$\mu_0 J_{z1} = \{ [C_1 a_1 r_{01} z / r^3] [F4] [\ln \cosh(z/D_1)] \\ - [C_1 / D_1] [F1] [\tanh(z/D_1)] \} \{ p + pq [\tanh^2(z/D_2)] \} \\ + \{ \{ C_1 [F1] - [C_1 a_1 r_{01} \rho^2 / r^3] [F4] \} [\ln \cosh(z/D_1)] \\ - C_2 \rho [\tanh(\rho_{02}/\rho)]^{a_2} - C_3 \rho [\tanh(\rho_{03}/\rho)]^{a_3} - C_4 \rho \} \\ \{ (2pq/D_2) [\tanh(z/D_2)] [\operatorname{sech}^2(z/D_2)] \} \\ \mu_0 J_{z2} = \{ [C_1 a_1 r_{01} z / r^3 (1 - 3\rho^2 / r^2)] [F4] - [C_1 a_1 r_{01}^2 \rho^2 z / r^6] [F5] \\ - [2C_1 a_1 r_{01}^2 \rho^2 z / r^6] [F3] \} [\ln \cosh(z/D_1)] + \{ - [C_1 / D_1] [F1] \\ + [C_1 r_{01} \rho^2 / D_1 r^3] [F4] \} [\tanh(z/D_1)] \} \{ p + pq [\tanh^2(z/D_2)] \} \\ + \{ \{ [C_1 a_1 r_{01} \rho^2 / r^3] [3\rho^2 / r^2 - 4] [F4] \}$$

$$\begin{aligned}
& + [C_1 a_1 (a_1 - 1) r_{01}^2 \rho^4 / r^6] [F5] + C_1 [F1] + [2C_1 a_1 r_{01}^2 \rho^4 / r^6] [F3] \} [\ln \cosh(z/D_1)] \\
& - 2C_2 \rho [\tanh(\rho_{02}/\rho)]^{a_2} + C_2 a_2 \rho_{02} [\tanh(\rho_{02}/\rho)]^{a_2-1} [\operatorname{sech}^2(\rho_{02}/\rho)] \\
& - 2C_3 \rho [\tanh(\rho_{03}/\rho)]^{a_3} + C_3 a_3 \rho_{03} [\tanh(\rho_{03}/\rho)]^{a_3-1} [\operatorname{sech}^2(\rho_{03}/\rho)] - 2C_4 \rho \} \\
& \{ (2pq/D_2) [\tanh(z/D_2)] [\operatorname{sech}^2(z/D_2)] \}
\end{aligned}$$

The thin disc currents are:

$$\mu_0 J_\rho = + p(C_1 \rho / D_1^2) [F1] [\operatorname{sech}^2(z/D_1)]$$

$$\mu_0 J_{\phi 1} = [C_1 / (D_1^2)] [F1] [\operatorname{sech}^2(z/D_1)]$$

Figure Captions

Figure 1 (see figure)

Figure 2 (see figure)

Figure 3 (see figure)

Figure 4 - Plots of J_ϕ vs ρ for both the volume and disc currents. The volume currents are those corresponding to various values of z as indicated in the figure.

Figure 5 - Plots of $\ln \cosh(z/D_1)$ times: $\tanh^2(z/D_2)$ (curve 1), $\tanh(z/D_2)\text{sech}^2(z/D_2)$ (curve 2), $\tanh^2(z/D_2)\text{sech}^2(z/D_2)$ (curve 3), and $\text{sech}^4(z/D_2)$ (curve 4). The last function occurs only in the expression for J_ρ as a modulator of $\ln \cosh(z/D_1)$. Also shown for comparison is a plot of the disc current representation, $\text{sech}^2(z/D_1)$.

Figure 6 - Plots of $\tanh(z/D_1)$ times $\tanh^2(z/D_2)$ (curve 1), $\tanh(z/D_2)\text{sech}^2(z/D_2)$ (curve 2), and $\tanh^2(z/D_2)\text{sech}^2(z/D_2)$ (curve 3). Also shown for comparison is a plot of the disc current representation, $\text{sech}^2(z/D_1)$

Figure 7 (plots of F_1 , F_3 , and F_4 hyperbolic modulation functions of (r_{01}/r))
See appendix 2 for definitions of F_1 , F_3 and F_4 .

Figure 8 (see figure)

Figure 9 (see figure)

Figure 10 The Khurana(1997) plus O6 magnetospheric field plus added magnetopause field caused by termination by a solar wind oriented perpendicular to a non-tilted planetary dipole field plus rigid corotating sheet current.

Figure 11 Same as Figure 10.